

Electron Transfer in Electrical Tribocharging Using a Quantum Chemical Approach

Ekaterina Nikitina

Institute of Applied Mechanics, Russian Academy of Sciences, Moscow, 117562 Russia

Herbert Barthel and Mario Heinemann[^]

Wacker Chemie AG, Johannes Hess Strasse 24, Werk Burghausen, D-84489 Burghausen, Germany

E-mail: herbert.barthel@wacker.com

Abstract. Electrical tribocharging is a fundamental physicochemical phenomenon and the basis of electrophotographic development. Despite extensive study, a complete understanding of the mechanism—commonly referred to as electron or ion transfer—remains unclear. Using a quantum chemical (QCh) approach, we studied the electron charge transfer (ECT) as one possible atomic-scale mechanism of tribocharging. We also describe ECT for several systems based on two materials in contact (tribopairs). Methods of density function theory and time-dependent density function theory were applied to QCh modeling using a cluster approach. A series of energetic and charge characteristics at the atomic level were calculated: including the highest- and lowest-occupied molecular orbitals (respectively) and the Fermi levels of complex components in their individual (free) as well as contact states, before and after electron excitation, ECT-excited energy states, charge distribution in the complexes, and the dipole moments of the excited complexes with ECT. Correlations were evaluated between the transferred charges and dipole moments and between transferred charges and Fermi levels. Furthermore, we could show that the QCh analysis offers insight into the ranking of tribocharging agents based on their chemical nature. © 2009 Society for Imaging Science and Technology.

[DOI: 10.2352/J.ImagingSci.Technol.2009.53.4.040503]

INTRODUCTION

Electrophotography is an important and highly developed technology.^{1,2} Industry is particularly interested in and is intensively researching contact charging—the main phenomenon of the electrophotographic development process^{3–5}—involved in nonimpact, toner, and developer-based printing technologies. A large number of experimental and theoretical studies have been conducted and summarized in comprehensive reviews^{6–21} and yet the mechanism of contact electrification remains unclear. Electron and/or ion transfers have been proposed for the charging mechanisms. Both mechanisms are most likely involved in contact charging, and each of them can be investigated using different approaches.

Charge transfer (CT) can arise when two different materials come into contact with one another: either by mere

touch or by the sliding of one body over another. An equal charge of opposite polarity remains on the surfaces after their subsequent separation. It is commonly accepted that tribocharging is driven by the difference in work functions between the surfaces in contact.^{22,23} The work function of a material is defined as the minimum energy required for removing an electron from the Fermi level to free space. The Fermi level is properly defined as the energy corresponding to the maximum in the first derivative of the Fermi-Dirac distribution function for electrons in the solid.^{14–21,24}

Should two materials with different work functions come into contact, unequal Fermi levels of the two materials will level out, driven by the difference in potential. Electrons will flow from the material with the smaller work function to the material with the larger work function, i.e., from the material with the higher Fermi level to the material with the lower Fermi level (see Figure 1).^{20,21} The work functions of the materials can be experimentally determined. By comparing the work functions of the materials in contact, it is possible to characterize tribopairs and to establish a triboelectric series.^{3,20,21} However, it is difficult to reproduce even simple experiments due to variations in the ambient atmosphere, including dust, chemical impurities and humidity, and due to uncontrollable alterations of the surfaces during contact.^{4,25}

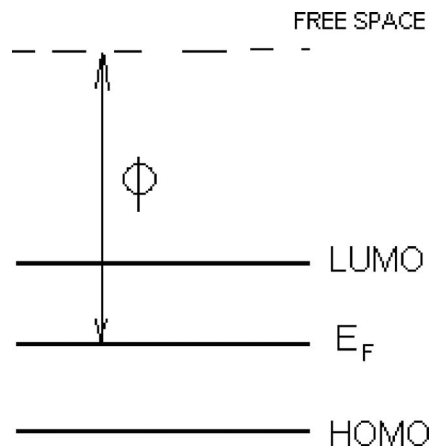


Figure 1. Energy diagram representing the relationship between work function (Φ), Fermi level (E_F), and HOMO and LUMO of molecular systems.

[^]IS&T Member.

Received Feb. 16, 2009; accepted for publication Apr. 16, 2009; published online Jun. 2, 2009.

1062-3701/2009/53(4)/040503/9/\$20.00.

An alternative approach involves the use of theory and computation to describe the contact charge. Several theoretical models are known. The electric field model is one of these. This model assumes that the electric field, originating from all toner particles, is equal to the electric field, which flows to all carrier particles.²⁶ There are also models for describing the surface state, i.e., the tribocharging of toner and carrier, in which the work functions are equilibrated and evaluated.^{14–21} Some models are based on orbital theory,⁹ whereby the electronic characteristics of tribopairs are investigated by means of numerical bond-structure calculations.^{27–30} The densities of states of the various species are calculated using various mathematical approaches to find the theoretical Fermi levels and, finally, to estimate work functions.

Quantum chemical (QCh) methods are the obvious choice for obtaining chemically significant information since they are particularly suited for determining the local properties of an investigated system,³¹ e.g., at the site of contact of the tribopartners. These methods were originally designed to describe finite systems. In practice, a representative cluster consisting of models of the two systems in contact is usually chosen.^{32,33} Because of the lack of translational periodicity, the electronic states of the noncrystalline systems investigated in this article cannot be described using Bloch's theory. In order to eliminate the artifacts caused by cluster boundaries, we must apply the fragment self-consistent field method,³⁴ neglecting diatomic differential overlap.

QCh modeling may provide atomic-scale descriptions of electron transfer during contact. Our goal is to determine an effect of frontier electronic states,³⁵ i.e., the highest-occupied molecular orbital (MO) (HOMO) and lowest-unoccupied molecular orbital (LUMO) of components and complexes with charge transfer. Positions of HOMO and LUMO levels can be calculated easily in the framework of quantum chemistry from the electronic eigenvalues of the clusters under study. Electron transfer from HOMO to LUMO located on different components of the charge transfer complex may result in tribocharging.

The position of Fermi levels is not clearly determined from electronic eigenvalue calculations. The Fermi level is a concept derived from the electronic structure of extended systems. Here we discuss its application to finite (molecular) systems. The canonical assumption is that the Fermi level of a molecule is situated near the center of the HOMO-LUMO gap.^{33,36} A computational model recently demonstrated how these conditions may arise in a cluster model of a molecular electronic junction.³³ Unequal Fermi levels at the contact area tend to level out through electron transfer, the charge flow continuing until Fermi levels reach equilibrium. This process yields Fermi levels of adsorption complexes with charge transfer in the excited states. Charges of opposite polarity are the result at the two contact surfaces (as models of materials), and these, too, can be easily calculated using the QCh method.

The current study was performed using *ab initio* density function theory (DFT)/time-dependent density function

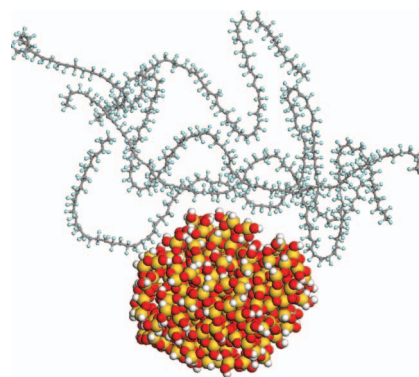


Figure 2. A schematic representation of the atomic-scale area of the contact surface between polymer chains and particle surfaces, i.e., for the SiO₂/PTFE system. Arrows mark contact areas.

theory (TDDFT) modeling of charge transfer states of several tribopairs, namely,

- (a) Silica and polytetrafluoroethylene (PTFE): (SiO₂/PTFE)
- (b) Alumina oxide and PTFE (Al₂O₃/PTFE)
- (c) Titanium dioxide and PTFE (TiO₂/PTFE)
- (d) Iron oxide and PTFE (Fe₂O₃/PTFE)
- (e) Primary amino-silane modified silica and PTFE (SiO₂-RNH₂/PTFE)
- (f) Tertiary amino-silane modified silica and PTFE (SiO₂-RN(CH₃)₂/PTFE)
- (g) Phosphonato-ester-silane modified silica (SiO₂-Si(CH₃)₂-CH₂CH₂CH₂-P(=O)×(OCH₂CH₃)₂) and PTFE (PE-silica/PTFE)
- (h) Silica and iron oxide (SiO₂/Fe₂O₃).

PTFE was chosen as a main reference for tribopairs since it is known to be negatively charged in most tribocontacts^{37–39} and has one of the highest work functions. In addition, the Fe₂O₃ and SiO₂ tribopair was studied since this system is of technological importance. Results from this study enabled us to predict a triboelectric series from the quantum chemistry first principles, using *ab initio* approaches.

COMPUTATIONAL MODELS AND APPROACHES

It is known that all contacts between surfaces that lead to tribocharging are local, and tribocharging occurs due to the microscopic and atomic-scale chemical structure (applies only to electrically insulating materials, i.e., those with high electrical resistance). Only some segments of a polymer chain will actually interact with the solid particle surface. These segments of the polymer in contact with the solid surface, consisting of several monomer units, form a surface adsorption layer with hindered torsional motion. A schematic representation of such contact is shown in Figure 2. In accordance with such a scheme, molecular cluster complexes may be used as appropriate models for the atomic-scale evaluation of contacts between macroscopic surfaces.

In the present study, we applied a cluster approach for modeling adsorption complexes and their components. The

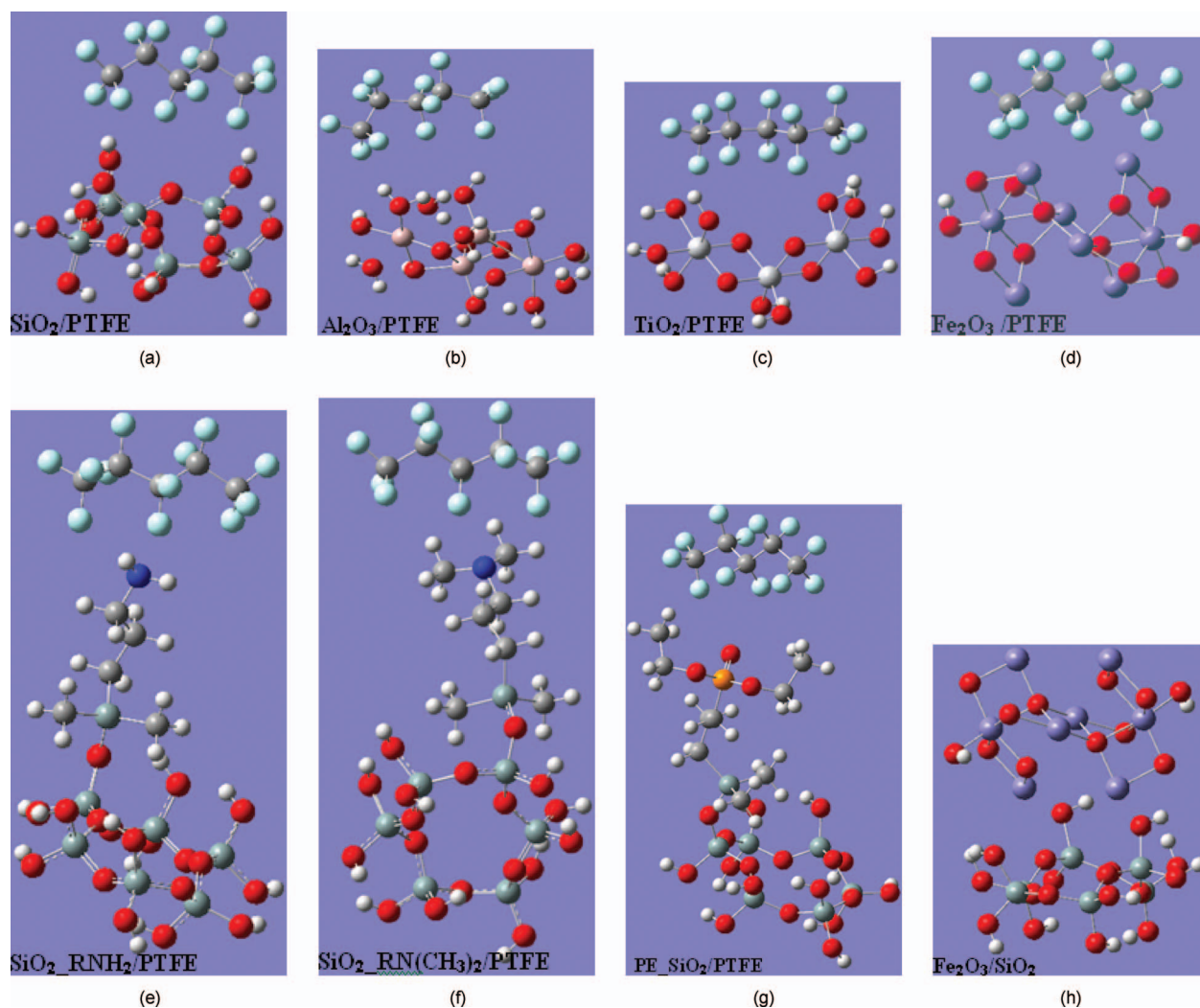


Figure 3. Summary of the equilibrated structures of the cluster models of adsorption complexes we examined.

area of contact was modeled by cluster complexes made up of polymer and/or solid particle surface components up to 100 atoms in size. Such models make it possible to perform expanded *ab initio* calculations within a reasonable time frame. Polymer components were represented by the corresponding oligomers, including several monomer units, and solid particle surface components were constructed as small clusters in order to reproduce the chemical nature of the solid's surface. Broken bonds at the surfaces were terminated with surface hydroxyl groups.

QCh-optimized cluster model structures of all the adsorption complexes we examined are presented in Figure 3. Later in this article, model clusters are denoted as A_i -PTFE where A_i is SiO_2 , Al_2O_3 , TiO_2 , Fe_2O_3 , $\text{SiO}_2\text{-RNH}_2$, $\text{SiO}_2\text{-RN}(\text{CH}_3)_2$, or PE-SiO_2 . Another model cluster ($\text{Fe}_2\text{O}_3\text{-SiO}_2$) was examined and its optimized structure presented in Fig. 3.

The model for the PTFE component was chosen as an oligomer of five tetrafluoroethylene monomer units. The silica model SiO_2 represents an amorphous cluster containing six silica-oxygen tetrahedrons. This SiO_2 cluster has 12 hydroxyl groups on the surface and is made up of 35 atoms.

The Al_2O_3 model represents a portion of an alumina oxide surface of 35 atoms. The Fe_2O_3 model is made up of 22 atoms in total, eight of which are iron. This last cluster reproduces a part of a ferrite surface area quite correctly, at a reasonable calculation effort. The TiO_2 cluster represents an anatase structure, consisting of 14 titanium atoms out of a total of 27. Cluster models of primary and tertiary-amino-silane modified silica were constructed on the basis of the SiO_2 cluster, whereby one of the surface hydroxyls has been replaced by an $-\text{O-Si}(\text{CH}_3)_2\text{-CH}_2\text{CH}_2\text{CH}_2\text{-NH}_2$ or $-\text{O-Si}(\text{CH}_3)_2\text{-CH}_2\text{CH}_2\text{CH}_2\text{-N}(\text{CH}_3)_2$ group, respectively. Phosphonato-ester-silane modified silica PE-SiO_2 consists of 71 atoms. It, too, is constructed on the basis of the SiO_2 cluster; in this case a surface hydroxyl group has been substituted with $-\text{O-Si}(\text{CH}_3)_2\text{-CH}_2\text{CH}_2\text{CH}_2\text{-P(=O)} \times (\text{OCH}_2\text{CH}_3)_2$.

Energy and charge characteristics of all these molecular systems and their adsorption complexes with and without CT were calculated in three steps,

- (1) First of all, the equilibrium geometries of all components of the adsorption complexes in the indi-

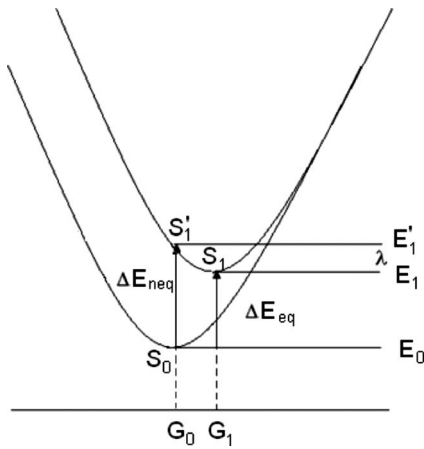


Figure 4. A scheme of nonequilibrium and equilibrium excitation and charge transfer state formation in tribo contact.

vidual (free) state were optimized. These computations were carried out with DFT with B3LYP functional and aug-cc-pVTZ basis set implemented in the GAUSSIAN⁰³ package. Though this method is very time consuming, it can provide highly accurate calculations. The computations yielded data on HOMO and LUMO energy levels and corresponding Fermi levels, as well as on the charge distributions across all the atoms of individual components of the adsorption complexes we studied.

- (2) Next, we constructed and equilibrated adsorption complexes using these optimized structures. The same DFT/B3LYP/aug-cc-pVTZ method was used. Ground states S_0 without CT were modeled for all complexes, giving HOMO and LUMO values of these adsorption complexes as well as important information concerning the location of HOMO and LUMO electron densities of the components within the complexes.
- (3) Previous calculations were then substituted for TD-DFT with the same functional and basis set for all model complexes. In this way, the lowest excited state (S_1) with CT was obtained, in which electron transfers from occupied MOs to unoccupied MO proceed owing to contact or friction excitation. A scheme of such an excitation is shown in Figure 4. Electron excitation after contact causes the components of adsorption complexes to increase their orbital energy from the ground state S_0 , in which the components of the complexes are not charged to the excited state S'_1 . Upon excitation, charge transfer is at first generated for geometries corresponding to ground states. After that, S_1 level optimized geometries are created. This occurs because the motion of electrons is much faster than the motion of the heavy nuclei of the atoms. As a result, non-equilibrium excitations and CT are the first to take place, and only after a lag time do the systems arrive at equilibrated CT excited states complete with

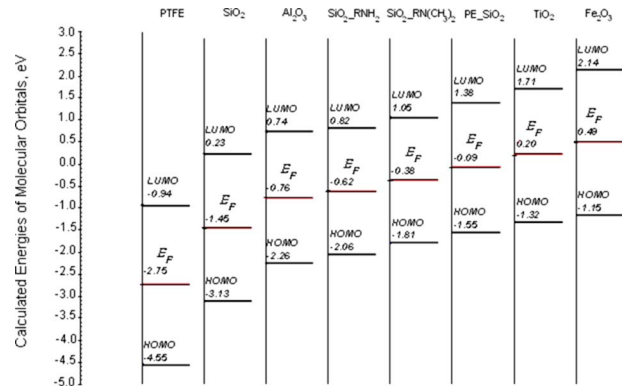


Figure 5. Summary of calculated HOMO and LUMO energies and Fermi levels (E_F) for single components of A_1 -PTFE.

intramolecular reorganization of the nuclei and charged components of the complexes.

Electron excitation therefore occurs in two stages, each of which must be calculated separately: a first nonequilibrium step and a second step described using equilibrium TDDFT approaches. In this way, the charge distributions across the atoms and components of each complex were calculated. The energies of nonequilibrium and equilibrium CT can be represented accordingly to the following equations (see Fig. 4):

$$\Delta E_{\text{neq}} = E'_1 - E_0 = \Delta E_{\text{eq}} + \lambda, \quad (1)$$

$$\Delta E_{\text{eq}} = E_1 - E_0, \quad (2)$$

where ΔE_{neq} is the energy of nonequilibrium CT $S_0 \rightarrow S'_1$, ΔE_{eq} is the energy of equilibrium CT $S_0 \rightarrow S_1$, E_0 is the energy of the ground state S_0 of the complex without CT (calculated in DFT approach for the ground state DFT-optimized geometry G_0), E'_1 is the energy of nonequilibrium excited state S'_1 with CT (calculated in TDDFT for ground state DFT-optimized geometry G_0), E_1 is the energy of equilibrium excited state S_0 with CT (calculated in TDDFT for TDDFT-optimized geometry G_1), and λ is the energy of structural reorganization from nonequilibrium to equilibrium excited state with CT. An analogical introduction of reorganization energy was provided by Nikitina et al.⁴⁰

Calculating the equilibrium geometries of adsorption complex components in their individual states, we could therefore make a prediction of the relative charge exchange between the different materials studied. On the basis of the quantum-chemically obtained data, we ranked the components in the adsorption complexes into a triboelectric series.

RESULTS AND DISCUSSION

Calculated energy levels E_{HOMO} and E_{LUMO} of HOMO and LUMO and their corresponding Fermi levels, which were estimated as the differential between E_{HOMO} and E_{LUMO} for all single components of the various complexes of A_1 -PTFE, are presented in Figure 5, where A_i is SiO₂, Al₂O₃, TiO₂,

Table I. Summary of calculated Fermi levels, HOMO, and LUMO energy levels for components of A_i -PTFE and Fe_2O_3 - SiO_2 complexes in free (individual) states.

A_i component	E_{HOMO} (eV)	E_{LUMO} (eV)	E_{F} (eV)	$E_{\text{HOMO_PTFE}}-E_{\text{LUMO_}A_i}$ (eV)	$E_{\text{HOMO_}A_i}-E_{\text{LUMO_PTFE}}$ (eV)
SiO_2	-3.13	0.23	-1.45	-4.78	-2.19
Al_2O_3	-2.26	0.74	-0.76	-5.29	-1.32
SiO_2 -RNH ₂	-2.06	0.82	-0.62	-5.37	-1.12
SiO_2 -RN(CH ₃) ₂	-1.81	1.05	-0.38	-5.6	-0.87
PE- SiO_2	-1.55	1.38	-0.09	-5.93	-0.61
TiO_2	-1.32	1.71	0.20	-6.26	-0.38
Fe_2O_3	-1.15	2.14	0.49	-6.69	-0.21
PTFE	-4.55	-0.94	-2.75		

Complex	$E_{\text{HOMO_SiO}_2}-E_{\text{LUMO_Fe}_2\text{O}_3}$ (eV)	$E_{\text{HOMO_Fe}_2\text{O}_3}-E_{\text{LUMO_SiO}_2}$ (eV)
Fe_2O_3 - SiO_2	-5.27	-1.38

Fe_2O_3 , SiO_2 -RNH₂, SiO_2 -RN(CH₃)₂, or PE- SiO_2 . These data, together with energy differences $E_{\text{HOMO_PTFE}}-E_{\text{LUMO_}A_i}$ and $E_{\text{HOMO_}A_i}-E_{\text{LUMO_PTFE}}$ are summarized in Table I. It is well established that PTFE has one of the strongest negative tribocontact charge capacities known. The positive charge-ability of the other components was therefore examined against PTFE. Additionally, $E_{\text{HOMO}}-E_{\text{LUMO}}$ for the system Fe_2O_3 - SiO_2 is presented in Table I.

During electron transfer from HOMO to LUMO, which are located at different components within A_i -PTFE complexes, electrons—under triboexcitation—will move from the component with the higher Fermi level (A_i) to the component with the lower Fermi level (PTFE). Therefore, it is sufficient to calculate the HOMO and LUMO energy levels for the individual tribocomponents in order to conclude that charges of opposite polarity will arise on the two interacting components of A_i -PTFE complexes. Negative charges will be located on the component with the lower Fermi level, i.e., PTFE, and positive charges will be located on the component with the higher Fermi level i.e., A_i .

The following sequence can be deduced from the results of this study, correlating with increasing positive charge-ability of the tribocomponents in contact with PTFE.

$\text{SiO}_2 < \text{Al}_2\text{O}_3 < \text{primary amino-silane modified SiO}_2 < \text{tertiary amino-silane modified SiO}_2 < \text{phosphonato-ester-silane modified SiO}_2 < \text{TiO}_2 < \text{Fe}_2\text{O}_3$.

The triboelectric series as determined above from the HOMO and LUMO levels approximates the empirical data. The data presented in this article generally agree with experimental data, but there is not a perfect match. There is some disconnect with the position of alumina and titania, with regard to some empirical data, where the order of negative charge was found to be silica > titania > alumina.^{20,21} The reason for this discrepancy can be in a possibility of ion transfer, the consideration of which is out of framework of our study. However, ion transfer could also be involved in

tribocharging for some of these materials, particularly for alumina and titania chemistry of which is not totally covalent.

It is clear from the HOMO and LUMO analyses of the Fe_2O_3 / SiO_2 pair that during triboformation of CT states, electrons will move from the Fe_2O_3 to the SiO_2 component. In other words, in the CT state, Fe_2O_3 particles will be positively charged and the SiO_2 particles negatively charged.

The charge distributions across atoms of the individual components of A_i -PTFE complexes were also initially calculated. Each of those components is neutrally charged in the individual free state. These data were used as a reference and are included in a discussion of charge distributions in corresponding CT complexes below.

Highly illustrative results were obtained at the second step of the modeling, where ground states S_0 without CT were computed for all the complexes we have examined. In this step, we calculated MO levels and the distributions of electron density over MO of the components of the various A_i -PTFE adsorption complexes, as well as for the complex Fe_2O_3 - SiO_2 . The calculated HOMO and LUMO electron density distributions for the A_i -PTFE and Fe_2O_3 - SiO_2 adsorption complexes before CT were visualized by GAUSSIAN VIEWER and are presented in Figure 6.

These results gave us important information concerning the location of HOMO and LUMO in specific complex components. As seen from Figure 6, HOMO densities of the complexes are located at the A_i component in all cases, particularly in the case of PE- SiO_2 at the phosphonato-ester group. LUMOs of all complexes are located at the PTFE component. It should be possible to transfer electrons located within the HOMO by triboexcitation. Components bearing the LUMO are able to receive electrons. In the case of the A_i -PTFE complexes we studied, tribocharging can occur if electrons are transferred from HOMO located within the A_i component to LUMO located within PTFE.

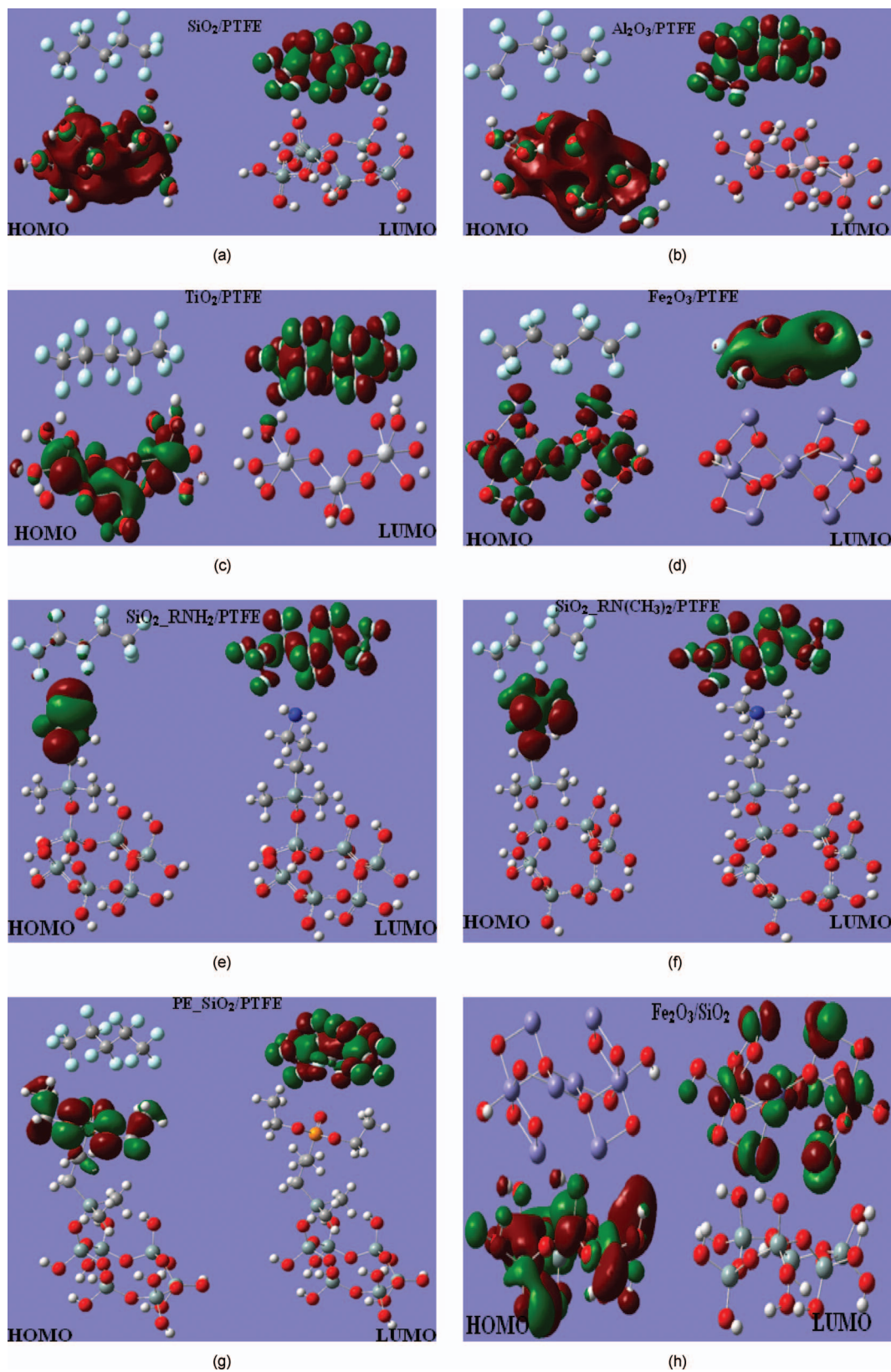


Figure 6. Summary of calculated HOMO and LUMO electron density distributions for A_1 -PTFE adsorption complexes before charge transfer.

Table II. Summary of HOMO and LUMO energy levels of A_i -PTFE and Fe_2O_3 - SiO_2 adsorption complexes.

A_i component	E_{HOMO}, A_i -PTFE complex (eV)	E_{LUMO}, A_i -PTFE complex (eV)
SiO_2	-3.12	-0.92
Al_2O_3	-2.25	-0.91
SiO_2 - RNH_2	-2.04	-0.91
SiO_2 - $\text{RN}(\text{CH}_3)_2$	-1.84	-0.89
PE- SiO_2 -PTFE	-1.57	-0.92
TiO_2	-1.35	-0.90
Fe_2O_3	-1.21	0.87
Complex	$E_{\text{HOMO}}, \text{Fe}_2\text{O}_3$ - SiO_2 (eV)	$E_{\text{LUMO}}, \text{Fe}_2\text{O}_3$ - SiO_2 (eV)
Fe_2O_3 - SiO_2	-1.18	0.21

In addition, the calculated HOMO and LUMO electron density distributions for the adsorption complex Fe_2O_3 - SiO_2 before CT are presented in Fig. 6. Here, we can see that the HOMO of the Fe_2O_3 - SiO_2 complex is located on the Fe_2O_3 component and that the LUMO is located on the SiO_2 component. Therefore, electron excitation and transfer may occur in this system by electron transfer from the Fe_2O_3 component to the SiO_2 component.

We also calculated the values of HOMO and LUMO energy levels of the adsorption complexes we examined during the second step of the modeling process. These values are summarized in Table II.

Comparing the results in Table II with the HOMO and LUMO levels computed for the various individual components, it is obvious that the HOMO energy values of the complexes are close to the HOMO energies of the corresponding individual A_i components. Likewise, LUMO energy values in all complexes approximate the LUMO energy of PTFE. This is an evidence that within a complex, the A_i component is responsible for HOMO formation and PTFE for LUMO formation.

The third step of the modeling process consisted of calculating the energy characteristics ΔE_{neq} , ΔE_{eq} , and λ for the excited MO states of A_i -PTFE complexes with CT according to the scheme presented in Figure 4. Corresponding data are collected in Table III.

A comparison of the energy characteristics of the various A_i components and their ability to form excited states is presented in Table III. The lower the values of ΔE_{neq} , ΔE_{eq} , and λ , the easier triboexcitation may occur. On the basis of these data, the A_i components may be arranged as the following tribpairs with PTFE: $\text{SiO}_2 < \text{Al}_2\text{O}_3 < \text{primary amino-silane modified SiO}_2 < \text{tertiary amino-silane modified SiO}_2 < \text{phosphonato-ester-silane modified SiO}_2 < \text{TiO}_2 < \text{Fe}_2\text{O}_3$.

This sequence is in concordance with that obtained from the HOMO and LUMO data for individual A_i components.

Table III. Summary of calculated energies of nonequilibrium and equilibrium CT-excited states and the corresponding energies of intramolecular reorganization for A_i -PTFE complexes and for the Fe_2O_3 - SiO_2 complex.

Complex	ΔE_{eq} (eV)	ΔE_{neq} (eV)	λ (eV)
SiO_2 -PTFE	5.24	6.16	0.92
Al_2O_3 -PTFE	4.66	5.26	0.60
SiO_2 - RNH_2 -PTFE	4.27	4.76	0.49
SiO_2 - $\text{RN}(\text{CH}_3)_2$ -PTFE	2.23	2.54	0.31
PE- SiO_2 -PTFE	2.03	1.79	0.24
TiO_2 -PTFE	1.89	1.71	0.18
Fe_2O_3 -PTFE	1.68	1.54	0.14
Fe_2O_3 - SiO_2	1.92	1.71	0.21

At this step, the charge distributions across all atoms of the various adsorption complexes were calculated for excited equilibrium states with CT. As an example, we cite the distribution for PE- SiO_2 /PTFE, together with distributions received for the corresponding individual components of this complex during the first stage of modeling (see above). The corresponding distributions are presented in Figure 7 and reveal a similar tendency as already described above.

Plotting the data for CT complexes and for single components, we can conclude that the partial charges on all atoms of the PTFE component become more negative compared to charges of the same atoms at a free PTFE surface. The sum of these partial negative charges resulting from triboexcitation and intermolecular CT complex formation is the total transferred charge. The partial charges on atoms of PE- SiO_2 changed according to their location within the complex. In contrast to the core atoms of the SiO_2 cluster, where the charges do not change significantly, the charges at the surface phosphonato-ester group became noticeably more positive. It can be assumed that these very atoms participate in the CT process. HOMO and LUMO electron density distributions confirm this as well, as can be seen in Fig. 5. Indeed, we see here that the HOMO for this system is located on the phosphonato-ester group.

All components of A_i -PTFE tribocomplexes maintain zero charge in the isolated state. After triboexcitation and CT, both components of each complex acquire partially transferred charges. The total charges transferred were calculated at the third stage for each complex in its equilibrium CT state as the sum of the partial charges for each component atom. Values of the total transferred charges are summarized in Table IV, together with the calculated dipole moments for excited complexes with CT.

The calculated values of transferred charges are very important. First of all, these data reveal that the charge transfer from one component to another occurs in triboexcited states of A_i -PTFE. Second, they are important because the magnitude of these transferred charges characterizes the ability of tribocomponents to receive or to lose charges. On the basis of the results presented in Table IV, we can arrange the

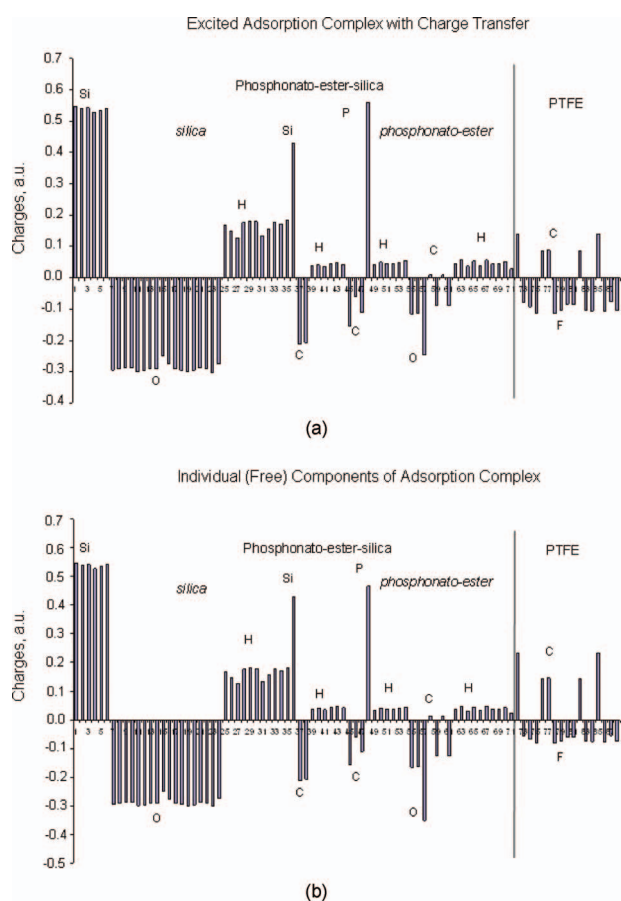


Figure 7. Charge distributions (a) across atoms of the PE_SiO₂_PTFE adsorption complex in the excited equilibrium state with charge transfer and (b) across atoms of individual PE_SiO₂ and PTFE components.

Table IV. Charge distribution (transferred or partial charge) across components in the various A_i_PTFE complexes at the equilibrium CT-excited state.

Complex	Charge on A _i (a.u.)	Charge on PTFE (a.u.)	Dipole moment of complex D
SiO ₂ _PTFE	0.95	-0.95	6.41
Al ₂ O ₃ _PTFE	1.16	-1.16	7.32
SiO ₂ _RNH ₂ _PTFE	1.20	-1.20	7.87
SiO ₂ _RN(CH ₃) ₂ _PTFE	1.48	-1.48	8.49
PE_SiO ₂ _PTFE	1.52	-1.52	9.58
TiO ₂ _PTFE	1.67	-1.67	10.25
Fe ₂ O ₃ _PTFE	1.84	-1.84	12.68
Fe ₂ O ₃ _SiO ₂	1.58	-1.56	9.23

A_i components in the following sequence: SiO₂ < Al₂O₃ < primary amino-silane modified SiO₂ < tertiary amino-silane modified SiO₂ < phosphonato-ester-silane modified SiO₂ < TiO₂ < Fe₂O₃.

As can be seen in Table IV, all the excited complexes with CT have rather large dipole moments. Indeed, it is known that a high dipole moment indicates a charge partition in the molecular system. The greater the transfer of charge that occurs, the larger the value of the dipole moment

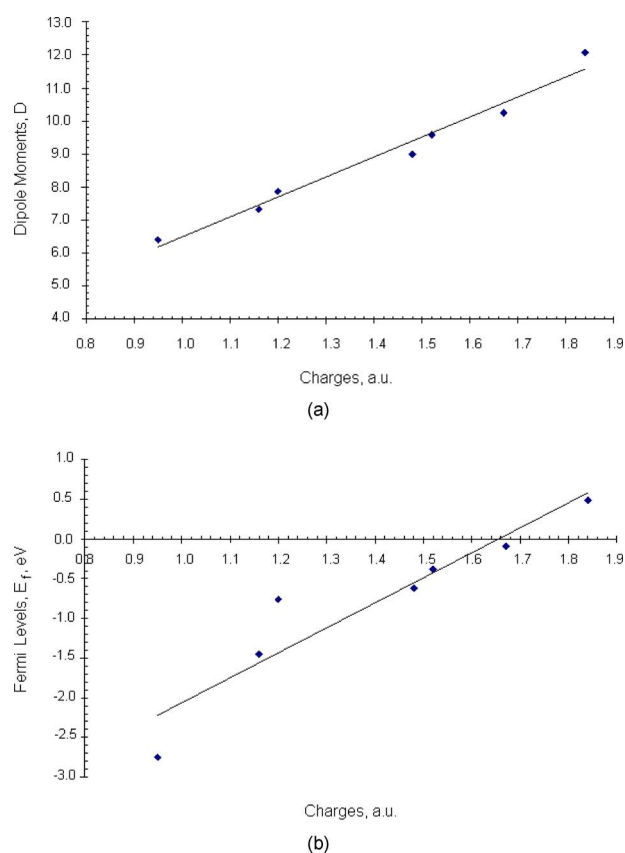


Figure 8. Correlation functions (a) between transferred charges and dipole moments of the complexes in the excited state with charge transfer and (b) between transferred charges of the complexes in the excited state with charge transfer and calculated Fermi levels for the complexes at the ground state without charge transfer.

of its corresponding molecular system will be. Correlations were obtained between transferred charges (for excited states with CT) and dipole moments of the various complexes, as well as between transferred charges and Fermi levels (as calculated for the ground states of uncharged complexes) (see Figure 8). There is a linear dependence between the modeled dipole moments and modeled transferred charge. The amount of transferred charge depends on the Fermi levels and reveals that the modeling is consistent with Fermi levels driving charge separation and thus potentially driving triboelectric charging.

CONCLUSIONS

This study was devoted to the quantum chemical investigation of atomic-scale mechanisms and atomic-scale characteristics of tribocharging phenomena. To our knowledge, this is the first attempt at applying highly accurate *ab initio* calculations in order to arrange the components into tribopairs. We hope that the outlined approach developed within this study will be helpful for future computations of the components of tribopairs.

We investigated eight tribopairs, namely, SiO₂/PTFE, Al₂O₃/PTFE, TiO₂/PTFE, Fe₂O₃/PTFE, primary-amino-silane modified SiO₂/PTFE, and tertiary-amino-silane modified SiO₂/PTFE, phosphonato-ester-silane modified

Table V. Quantum-chemically predicted triboelectric series.

Most positive
Fe ₂ O ₃
TiO ₂
SiO ₂ -Si(CH ₃) ₂ -(CH ₂) ₃ P(=O)(OCH ₂ CH ₃) ₂
SiO ₂ -RN(CH ₃) ₂
SiO ₂ -RNH ₂
Al ₂ O ₃
SiO ₂
PTFE
Most negative

SiO₂/PTFE, and Fe₂O₃/SiO₂. To this end, we have computed and analyzed the quantum chemical characteristics of triboexcitation for these adsorption complexes, including (i) HOMO and LUMO energies, (ii) energies of Fermi levels, (iii) dipole moments, and (iv) charge distributions across atoms and components of triboadsorption complexes (both in individual states and in complexes), (v) energy characteristics such as energies of nonequilibrium and equilibrium excitation with charge transfer, and (vi) the corresponding energies of intramolecular reorganization attendant to charge transfer.

With these data, we have predicted a quantum-chemically based triboelectric series as presented in Table V. It is our opinion that our ability to establish a quantum-chemically based triboelectric series is one of the most important outcomes of our current study.

REFERENCES

- R. A. Myers and J. C. Tamilus, "Introduction to topical issue on non-impact printing technologies", *IBM J. Res. Dev.* **28**, 234 (1984).
- M. H. Lee, J. E. Ayala, B. D. Grant, W. Imano, A. Jaffe, M. R. Latta, and S. L. Rice, "Technology trends in electrophotography", *IBM J. Res. Dev.* **28**, 241 (1984).
- M. Akbi and A. Lefort, "Work function measurements of contact materials for industrial use", *J. Phys. D* **31**, 1301 (1998).
- H. Barthel and M. Heinemann, in *Recent Progress in Toner Technologies*, edited by G. Marshall (IS&T, Springfield, VA, 1997), p. 117.
- Encyclopedia Britannica* (Encyclopedia Britannica, Chicago, IL, 1955), Vol. **8**, p. 169.
- B. A. Kwetkus and K. Sattler, "Contact charging of oxidized metal powders", *Int. J. Mod. Phys. B* **82**, 87 (1991).
- J. Lowell, "Bidirectional charge transfer in repeat contacts to polymers", *J. Electrostat.* **20**, 233 (1987).
- A. R. Akande and J. Lowell, "Charge transfer in metal/polymer contacts", *J. Phys. D* **20**, 565 (1987).
- A. F. Diaz and J. Guay, "Contact charging of organic materials: Ion vs. electron transfer", *IBM J. Res. Dev.* **37**, 249 (1993).
- C. B. Duke and T. J. Fabish, "Charge-induced relaxation in polymers", *Phys. Rev. Lett.* **37**, 1075 (1976).
- T. J. Fabish and C. B. Duke, "Molecular charge states and contact charge exchange in polymers", *J. Appl. Phys.* **48**, 4256 (1977).
- C. B. Duke and T. J. Fabish, "Contact electrification of polymers: A quantitative model", *J. Appl. Phys.* **49**, 315 (1978).
- T. J. Fabish and C. B. Duke, "Charge transfer in metal/polymer contacts and the validity of contact charge spectroscopy", *J. Appl. Phys.* **51**, 1247 (1980).
- J. H. Anderson, "A comparison of experimental data and model predictions for tribocharging of two-component electrophotographic developers", *J. Imaging Sci. Technol.* **38**, 378 (1994).
- J. H. Anderson, "Surface state analysis of tribocharging data for several toners using a set of reference carriers", *J. Imaging Sci. Technol.* **43**, 460 (1999).
- J. H. Anderson, "Surface state analysis of tribocharging data: Effect of carbon black", *J. Imaging Sci. Technol.* **44**, 129 (2000).
- G. S. P. Castle and L. B. Schein, "General model of sphere-sphere insulator contact electrification", *J. Electrostat.* **36**, 165 (1995).
- E. J. Gutman and G. C. Hartmann, "Study of the conductive properties of two-component xerographic develop materials", *J. Imaging Sci. Technol.* **36**, 335 (1992).
- L. H. Lee, "A surface interaction model for triboelectrification of toner-carrier pair", *Photograph. Sci. Eng.* **22**, 228 (1978).
- R. P. N. Veregin, M. N. V. McDougall, M. S. Hawkins, C. Vong, and V. Skorokhod, "A bidirectional acid base charging model for triboelectrification: Part 1. Theory", *J. Imaging Sci. Technol.* **50**, 282 (2006).
- R. P. N. Veregin, M. N. V. McDougall, M. S. Hawkins, C. Vong, and V. Skorokhod, "A bidirectional acid base charging model for triboelectrification: Part 2. Experimental verification by inverse gas chromatography and charging of metal oxides", *J. Imaging Sci. Technol.* **50**, 288 (2006); P. Brandl, Y. Amano, A. Inoue, M. Kaneeda, S. Hasenzahl, M. Maier, M. Moerters, and R. E. Johnson, "Evolution and regulatory impact of fumed inorganic materials in toners", *Proc. IS&T's NIP24* (IS&T, Springfield, VA, 2008) p. 1.
- H. B. Michaelson, "Work function of the elements", *J. Appl. Phys.* **21**, 536 (1950).
- J. Lowell and A. C. Rose-Innes, "Contact electrification", *Adv. Phys.* **29**, 947 (1980).
- W. F. Leonard and T. L. Martin, *Electronic Structure and Transport Properties of Crystals* (R.E. Krieger Pub. Co., Huntington, NY, 1980), ISBN: 0882759868.
- J. Lowell and A. Brown, "Contact electrification of chemically modified surfaces", *J. Electrostat.* **21**, 69 (1988).
- T. Kurita, "Charge saturation mechanisms for mono-, and two-component electrophotographic developers", *Electrophotography* **26**, 126 (1987).
- W. A. Harrison, "Bond orbital model and the properties of tetrahedrally coordinated solids", *Phys. Rev. B* **8**, 4487 (1973).
- S. Sugihara, I. Yonekura, N. Asaba, and R. Sekine, "Electronic structure for wetting of BaTiO₃ with electrode metals", *J. Korean Phys. Soc.* **32**, S1119 (1998).
- K. Akagi, R. Tamura, and M. Tsukada, "Electronic structure of helically coiled carbon nanotubes: Relation between the phason lines and energy band features", *Phys. Rev. B* **53**, 2114 (1996).
- L. Chico, V. H. Crespi, L. X. Benedict, S. G. Louie, and M. L. Cohen, "Pure carbon nanoscale devices: Nanotube heterojunctions", *Phys. Rev. Lett.* **76**, 971-974 (1996).
- L. G. Bulusheva, A. V. Okotrub, D. A. Romanov, and D. Tomanek, "Electronic structure of (n,0) zigzag carbon nanotubes: Cluster and crystal approaches", *J. Phys. Chem. A* **102**, 975 (1998).
- K. Kadas and S. Kugler, "Properties of midgap states in doped amorphous silicon and carbon", *J. Optoelectron. Adv. Mater.* **4**, 455 (2002).
- K. Sohlberg and N. Vedova-Brook, "Excursions of the Fermi level from the HOMO-LUMO gap in finite systems", *J. Comput. Theor. Nanosci.* **1**, 256 (2004).
- G. Gyoergy, G. G. Ferenszy, J.-L. Rivail, P. R. Surjan, and G. Naray-Szabo, "NDDO fragment self-consistent field approximation for large electronic systems", *J. Comput. Chem.* **13**, 830-837 (1992).
- K. Fukui, in *Nobel Lectures in Chemistry*, edited by B. G. Malmström (World Scientific, London, 1993).
- H. W. Gibson, "Control of electrical properties of polymers by chemical modification", *Polymer* **25**, 3 (1984).
- W. D. Greason, I. M. Oltean, Z. Kucerovsky, and A. C. Ieta, "Triboelectric charging between polytetrafluoroethylene and metals", *IEEE Trans. Ind. Appl.* **40**, 442-450 (2004).
- E. Nemeth, V. Albrecht, G. Schubert, and F. Simon, "Polymer triboelectric charging: dependence on thermodynamic surface properties and relative humidity", *J. Electrostat.* **58**, 3 (2003).
- R. J. Nash and R. N. Muller, in *Recent Progress in Toner Technologies*, edited by G. Marshall (IS&T, Springfield, VA, 1997), p. 267.
- E. A. Nikitina, A. V. Odinokov, F. V. Grigoriev, M. V. Basilevsky, A. A. Khlebunov, V. A. Sazhnikov, and M. V. Alfimov, "Molecular simulation of solvent-induced Stokes shift in absorption/emission spectra of organic chromophores", *J. Phys. Chem. B* **111**, 3953 (2007).